Fault Location Algorithm for Use with Current Differential Protective Relays of Double–Circuit Line

Eugeniusz Rosolowski, *Senior Member, IEEE*, Jan Izykowski, *Senior Member, IEEE*,
and Murari M. Saha, *Senior Member, IEEE*

Abstract--**A new algorithm designated for locating faults on a double-circuit line is presented. It is assumed that the fault location function is incorporated into the current differential relay at the particular line end. Besides three-phase currents measured synchronously at both line ends, which are utilized by the protective relays, the fault locator is supplied with three-phase voltage from the local line terminal, and possibly with the zero-sequence current from the healthy parallel line. Formulation of the fault location algorithm is presented and the selected results of the performed ATP-EMTP based evaluation are delivered and discussed.**

Index Terms—**Algorithms, communication channels, coupled transmission lines, fault location, Global Positioning System, power system faults, power system simulation, protective relaying.**

I. INTRODUCTION

ACCURATE location of faults on overhead power lines for an inspection-repair purpose [1]–[5] is of vital importance for expediting service restoration, and thus for reducing outage time, operating costs and customer complains. A great variety of fault location algorithms [1]–[5] has been developed so far. Different availability of measurements is considered for them, i.e. one-end measurements, and much superior two-end, or multi-end measurements. The measurements at different line ends can be performed synchronously – with use of the GPS or other means for synchronizing digital measurements, or asynchronously.

This paper presents the new algorithm for locating faults on a double-circuit line, with use of the signals of current differential relays. Similar algorithm, however designated to locating faults on a single-circuit line only, has been presented in [4]. In this paper, as its innovative, the compensation for the mutual coupling of parallel lines is solved. In that respect it is considered that the healthy parallel line is in operation or switched off and grounded at both line ends.

This is considered here (Fig. 1) that the fault locator (FL) is incorporated into the current differential relay from the terminal AA. Besides three-phase currents $\{i_{AA}\}$, $\{i_{BA}\}$, measured synchronously by the differential relays (REL$_{AA}$, REL$_{BA}$) at both line ends (AA, BA), the fault locator is additionally supplied with a three-phase voltage $\{v_A\}$ from the local line terminal. Additionally, for compensating mutual coupling of the line circuits, possible use of the zero-sequence current i_{AB0} from the healthy parallel line, as the fault locator input signal, is considered as well. The compensation is also solved for the case with no signal from the healthy parallel line at the fault locator input.

The developed fault location algorithm is categorized to the impedance-based method and is formulated using phasors of symmetrical components of the measured three-phase quantities. For deriving the fault location algorithm, the fault loops relevant for different fault types are considered with use of the generalized fault loop model. The universal fault loop formula is derived in which the fault type is set with the respective coefficients.

With the aim of providing high accuracy for locating faults on long lines, the distributed parameter line model is utilized. Both, the voltage drop across the faulted line segment and also across the fault path resistance are determined with taking into account the distributed parameter line model.

After derivation of the fault location algorithm, its evaluation, with use of the signals from ATP-EMTP [6] simulations, is presented and discussed (Section IV).

II. FAULT LOCATION ALGORITHM

A. Generalized fault loop model

In this paper, use of incomplete two-end measurements to fault location is considered. Due to insufficient measurement data, instead of processing the signals of the individual symmetrical component type, the natural fault loops are considered. Thus, accordingly to the identified fault type, the single phase loop (for phase-to-ground faults) or inter-phase loop (for faults involving two or three phases) is considered.

In further considerations, the case of the fault locator FL (Fig.1) incorporated into the differential relay at bus AA is taken into account. The algorithm for the other case, i.e. for the fault locator incorporated into the relay at bus BA, can be formulated analogously.
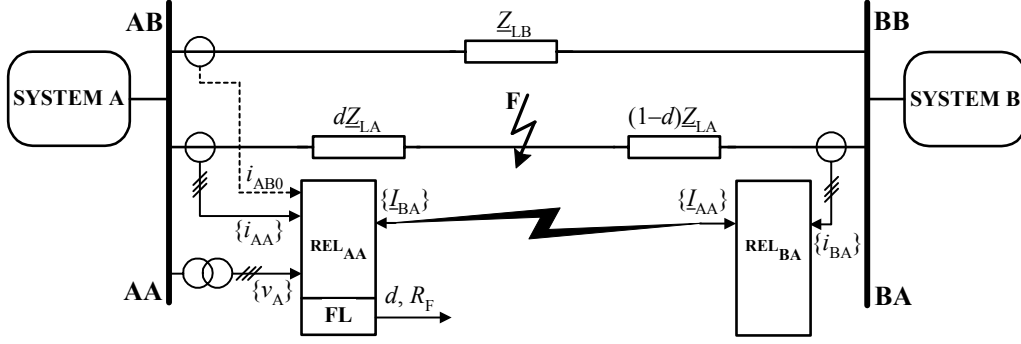
Fig. 1. Fault locator (FL) for a double-circuit line utilizing measurements of current differential relays REL$_{AA}$ and REL$_{BA}$ and additionally local measurements

The generalized fault loop model describes the fault loop seen from the line end AA, applying the following formula:

$$\underline{V}_{AFp}(d) - R_F \underline{I}_F = 0 \qquad (1)$$

where:

$\underline{V}_{AFp}(d_A)$ – fault loop voltage, composed accordingly to the fault type, which is obtained after an analytic transfer from the bus AA to the fault point F,

d – unknown distance, counted from bus AA to fault F (p.u.),

R_F – fault path resistance,

$\underline{I}_F$ – total fault current (fault path current).

B. Fault loop voltage at fault point

The transfer of the fault loop voltage from the bus AA to the fault point F is equivalent to subtracting the voltage drop across the faulted line section (part of the loop between the bus AA and the fault point F) from the original fault loop voltage at the bus AA. The transferred fault loop voltage can be composed as the following weighted sum of the respective symmetrical components:

$$\underline{V}_{AFp}(d_A) = \underline{a}_1 \underline{V}_{F1}(d) + \underline{a}_2 \underline{V}_{F2}(d) + \underline{a}_0 \underline{V}_{F0}(d) \qquad (2)$$

where the subscripts denoting a component type are as follows: 1 – positive-, 2 – negative-, 0 – zero-sequence,

$\underline{a}_1$, $\underline{a}_2$, $\underline{a}_0$ – weighting coefficients dependent on fault type, as gathered in Table I.

TABLE I. WEIGHTING COEFFICIENTS FOR COMPOSING SIGNAL (2)

FAULT TYPE	$\underline{a}_1$	$\underline{a}_2$	$\underline{a}_0$
a-g	1	1	1
b-g	$\underline{a}^2$	$\underline{a}$	1
c-g	$\underline{a}$	$\underline{a}^2$	1
a-b, a-b-g a-b-c, a-b-c-g	$1 - \underline{a}^2$	$1 - \underline{a}$	0
b-c, b-c-g	$\underline{a}^2 - \underline{a}$	$\underline{a} - \underline{a}^2$	0
c-a, c-a-g	$\underline{a} - 1$	$\underline{a}^2 - 1$	0
$\underline{a} = \exp(j2\pi/3)$; $j = \sqrt{-1}$			

The symmetrical components of voltages from (2) are determined as follows:

$$\underline{V}_{F1}(d) = \underline{V}_{A1} \cosh(\underline{\gamma}_{1LA}\ell d) - \underline{Z}_{c1LA}\underline{I}_{AA1}\sinh(\underline{\gamma}_{1LA}\ell d) \quad (3)$$

$$\underline{V}_{F2}(d) = \underline{V}_{A2} \cosh(\underline{\gamma}_{1LA}\ell d) - \underline{Z}_{c1LA}\underline{I}_{AA2}\sinh(\underline{\gamma}_{1LA}\ell d) \quad (4)$$

$$\underline{V}_{F0}(d) = \underline{V}_{A0} \cosh(\underline{\gamma}_{0LA}\ell d) - \underline{Z}_{c0LA}\underline{I}_{AA0}\sinh(\underline{\gamma}_{0LA}\ell d)$$
$$- d\underline{Z}_{0m}\underline{I}_{AB0} \qquad (5)$$

where:

$\underline{V}_{A1}$, $\underline{V}_{A2}$, $\underline{V}_{A0}$ – symmetrical components of voltage from the joint buses AA, AB,

$\underline{I}_{AA1}$, $\underline{I}_{AA2}$, $\underline{I}_{AA0}$ – symmetrical components of current at bus AA,

ℓ – length of the line (km),

$\underline{\gamma}_{1LA} = \sqrt{\underline{Z}'_{1LA}\underline{Y}'_{1LA}}$ – propagation constant of the line for the positive- sequence (negative-sequence),

$\underline{\gamma}_{0LA} = \sqrt{\underline{Z}'_{0LA}\underline{Y}'_{0LA}}$ – propagation constant of the line for the zero-sequence,

$\underline{Z}_{c1LA} = \sqrt{\underline{Z}'_{1LA}/\underline{Y}'_{1LA}}$ – characteristic impedance of the line for the positive-sequence (negative-sequence),

$\underline{Z}_{c0LA} = \sqrt{\underline{Z}'_{0LA}/\underline{Y}'_{0LA}}$ – characteristic impedance of the line for the zero-sequence,

$\underline{Z}'_{1LA} = R'_{1LA} + j\omega_1 L'_{1LA}$ – impedance of the line for the positive-sequence (negative-sequence) (Ω/km),

$\underline{Z}'_{0LA} = R'_{0LA} + j\omega_1 L'_{0LA}$ – impedance of the line for the zero-sequence (Ω/km),

$\underline{Y}'_{1LA} = G'_{1LA} + j\omega_1 C'_{1LA}$ – admittance of the line for the positive-sequence (negative-sequence) (S/km),

$\underline{Y}'_{0LA} = G'_{0LA} + j\omega_1 C'_{0LA}$ – admittance of the line for the zero-sequence (S/km),

R'_{1LA}, L'_{1LA}, G'_{1LA}, C'_{1LA} – resistance, inductance, conductance and capacitance of the line for the positive-sequence (negative-sequence) per km length,

R'_{0LA}, L'_{0LA}, G'_{0LA}, C'_{0LA} – resistance, inductance, conductance and capacitance of the line for the zero-sequence per km length,

$\underline{I}_{AB0}$ – zero sequence current from the healthy line circuit, considered as available for the fault locator or as estimated,

$\underline{Z}_{0m}$ – zero sequence mutual coupling line impedance.

The line parameters for the positive- and negative-sequence are identical and therefore they are uniformly denoted with '1' in the subscripts for both sequences.

C. Total fault current

Summing of phase currents (a, b, c in the subscripts for denoting phases) from both line ends (AA, BA in the subscripts) appears as the simplest way of determining the fault current in particular phases at the fault point:

$$\underline{I}_{Fa} = \underline{I}_{AAa} + \underline{I}_{BAa} \qquad (6)$$

$$\underline{I}_{Fb} = \underline{I}_{AAb} + \underline{I}_{BAb} \qquad (7)$$

$$\underline{I}_{Fc} = \underline{I}_{AAc} + \underline{I}_{BAc} \qquad (8)$$

Then, one can use these currents (6)–(8) for composing the total fault current, accordingly to the fault type. However, this way of the composing reveals as affected by the currents charging line shunt capacitances. This is so, since in (6)–(8) the currents from the line ends are summed, and not the currents flowing from both sides directly into to the fault point. On the way from the line ends (AA, BA) to the fault point (F) the currents, which are summed in (6)–(8), are lessened by the currents charging line shunt capacitances.

Taking into account the share of individual symmetrical components ($\underline{I}_{F1}$, $\underline{I}_{F2}$, $\underline{I}_{F0}$) in the total fault current ($\underline{I}_F$) one obtains [4]:

$$\underline{I}_F = \underline{a}_{F1}\underline{I}_{F1} + \underline{a}_{F2}\underline{I}_{F2} + \underline{a}_{F0}\underline{I}_{F0} \qquad (9)$$

where:

$\underline{a}_{F1}$, $\underline{a}_{F2}$, $\underline{a}_{F0}$ – share coefficients, dependent on fault type and the assumed preference with respect to using particular sequences.

The set of the share coefficients recommended for use when composing the total fault current (9) is presented in Table II. Different, alternative sets of the share coefficients [5] can be applied, however, the sets for which the zero-sequence is eliminated ($\underline{a}_{F0} = 0$) – as in Table II, is recommended here.

TABLE II. SHARE COEFFICIENTS FOR COMPOSING TOTAL FAULT CURRENT (9)

FAULT TYPE	$\underline{a}_{F1}$	$\underline{a}_{F2}$	$\underline{a}_{F0}$
a–g	0	3	0
b–g	0	$3\underline{a}$	0
c–g	0	$3\underline{a}^2$	0
a–b	0	$1-\underline{a}$	0
b–c	0	$\underline{a}-\underline{a}^2$	0
c-a	0	$\underline{a}^2-1$	0
a-b-g	$1-\underline{a}^2$	$1-\underline{a}$	0
b-c-g	$\underline{a}^2-\underline{a}$	$\underline{a}-\underline{a}^2$	0
c-a-g	$\underline{a}-1$	$\underline{a}^2-1$	0
a-b-c, a-b-c-g	$1-\underline{a}^2$	$1-\underline{a}$ *)	0

*) – there is no negative sequence component under these faults and the coefficient can be assumed as equal to zero

By taking the coefficients from Table II, use of the line parameters for the zero-sequence – which are considered as unreliable data, is avoided for determining the total fault current. This is advantageous from the fault location accuracy point of view.

One can notice that, when using the share coefficients proposed in Table II, the preference of using the negative-sequence over the positive-sequence is set for single-phase and phase-to-phase faults. This is also advantageous from the fault location accuracy point of view.

After detailed analysis performed, and also with taking into account that the zero-sequence can be eliminated [3]–[4], the total fault current can be expressed as:

$$\underline{I}_F = \frac{\underline{a}_{F1}\underline{M}_1 + \underline{a}_{F2}\underline{M}_2}{\cosh(\underline{\gamma}_{1LA}\ell(1-d))} \qquad (10)$$

where:

$$\underline{M}_i = \underline{I}_{BAi} + \underline{I}_{AAi}\cosh(\underline{\gamma}_{1LA}\ell) - \frac{\underline{V}_{Ai}}{\underline{Z}_{c1LA}}\sinh(\underline{\gamma}_{1LA}\ell)$$

The subscript i denotes: $i=1$ – positive-sequence or $i=2$ – negative-sequence quantities.

D. Fault location formula

Substitution of the total fault current (10) into the generalized fault loop model (1) gives:

$$\underline{V}_{AFp}(d) - R_F \frac{\underline{a}_{F1}\underline{M}_1 + \underline{a}_{F2}\underline{M}_2}{\cosh(\underline{\gamma}_{1LA}\ell(1-d))} = 0 \qquad (11)$$

where:

$\underline{V}_{AFp}(d)$ – the transferred fault loop voltage, defined in (2)–(5), with use of the weighting coefficients specified for different faults in Table I,

$\underline{M}_1$, $\underline{M}_2$ – quantities defined in (10), in which the coefficients from Table II are involved.

and finally:

$$\underline{V}_{AFp}(d)\cdot\cosh(\underline{\gamma}_{1LA}\ell(1-d)) - R_F(\underline{a}_{F1}\underline{M}_1 + \underline{a}_{F2}\underline{M}_2) = 0 \quad (12)$$

where:

$\underline{V}_{AFp}(d)$ – defined in (2)–(5), with use of the weighting coefficients specified for different faults in Table I,

$\underline{M}_1$, $\underline{M}_2$ – quantities defined in (10),

$\underline{a}_{F1}$, $\underline{a}_{F2}$ – share coefficients (Table II).

The derived fault location formula (12) is compact and covers different fault types, what requires setting the appropriate fault type coefficients, as provided in Table I and in Table II.

There are two unknowns in the fault location formula (12): distance to fault d and fault resistance R_F. After resolving (12) into the real and imaginary parts, one of the known numeric procedures for solving nonlinear equations can be applied. It has been checked that the Newton-Raphson iterative method is a good choice for that.

Applying the Newton-Raphson method, the start of iterative calculations can be performed with the initial values for the unknowns: d^0, R_F^0, denoted with the superscript 0

(iteration number: 0, as the starting point for the 1st iteration of the calculations). These values can be calculated from the fault location formula (12) adapted to the lumped line model with neglecting shunt capacitances. This can be accomplished by introducing to (12) the substitutions: $\cosh(x) \to 1$, $\sinh(x) \to x$, where x is an argument of the considered hyperbolic trigonometric function. As a result, one obtains the following simplified fault location formula:

$$\underline{V}_{Ap} - d^0 \underline{Z}_{1LA} \underline{I}_{AAp} - R_F^0 \underline{M}_{12}^0 = 0 \qquad (13)$$

with the fault loop voltage and current from the line end A, defined for the lumped line model with neglected shunt capacitances:

$$\underline{V}_{Ap} = \underline{a}_1 \underline{V}_{A1} + \underline{a}_2 \underline{V}_{A2} + \underline{a}_0 \underline{V}_{A0} \qquad (14)$$

$$\underline{I}_{AAp} = \underline{a}_1 \underline{I}_{AA1} + \underline{a}_2 \underline{I}_{AA2} + \underline{a}_0 \left(\frac{\underline{Z}_{0LA}}{\underline{Z}_{1LA}} \underline{I}_{AA0} + \frac{\underline{Z}_{0m}}{\underline{Z}_{1LA}} \underline{I}_{AB0} \right) \qquad (15)$$

where:

$$\underline{M}_{12}^0 = \underline{a}_{F1} \underline{I}_{AA1} + \underline{a}_{F2} \underline{I}_{AA2}$$

$$\underline{Z}_{1LA} = \underline{Z}'_{1LA} \ell, \quad \underline{Z}_{0LA} = \underline{Z}'_{0LA} \ell.$$

Resolving (13) into the real and imaginary parts, the following compact formula for the distance to fault, after eliminating the unknown fault resistance, is obtained:

$$d^0 = \frac{\text{real}(\underline{V}_{Ap}) \cdot \text{imag}(\underline{M}_{12}^0) - \text{imag}(\underline{V}_{Ap}) \cdot \text{real}(\underline{M}_{12}^0)}{\text{real}(\underline{Z}_{1LA} \underline{I}_{Ap}) \cdot \text{imag}(\underline{M}_{12}^0) - \text{imag}(\underline{Z}_{1LA} \underline{I}_{Ap}) \cdot \text{real}(\underline{M}_{12}^0)} \qquad (16)$$

Having calculated the distance to fault (16), one can calculate the other unknown, i.e. the fault resistance. As for example, from the real part of (13) one gets:

$$R_F^0 = \frac{\text{real}(\underline{V}_{Ap}) - d^0 \text{real}(\underline{Z}_{1LA} \underline{I}_{Ap})}{\text{real}(\underline{M}_{12}^0)} \qquad (17)$$

In practice, for the line lengths up to 150 km, the simple formulae (16)–(17) can be utilised. However, in order to assure high accuracy of fault location on longer lines, the Newton-Raphson solution of (12), resolved earlier into the real and imaginary parts, has to be applied. The results obtained from (16)–(17) are used for starting these iterative calculations.

III. FAULT LOCATION UNDER LACK OF ZERO-SEQUENCE CURRENT FROM HEALTHY PARALLEL LINE

Zero sequence current from the healthy parallel line (Fig. 1: the current i_{AB0}) is utilized for compensation of the mutual coupling of the line circuits. If this current is not provided for the fault locator it has to be estimated from available measurements. Such estimation is considered further in relation to equivalent circuit diagrams of the network with the double-circuit line, presented here as the lumped parameter element (Fig. 2–Fig. 3).

Considering the flow of zero-sequence currents (Fig. 2) one obtains the following formula for the zero-sequence current at the fault point F:

$$\underline{I}_{F0} = \frac{\underline{I}_{AA0} - \underline{P}_0 \underline{I}_{AB0}}{1 - d} \qquad (18)$$

where:

$$\underline{P}_0 = \frac{\underline{Z}_{0LB} - \underline{Z}_{0m}}{\underline{Z}_{0LA} - \underline{Z}_{0m}}.$$

In turn, for the incremental positive-sequence components (obtained by subtracting the pre-fault value from the fault value) one obtains after considering the circuit of Fig. 3:

$$\underline{I}_{F1} = \frac{\Delta \underline{I}_{AA1}}{\underline{k}_{F1}} = \frac{\underline{I}_{AA1} - \underline{I}_{AA1}^{pre}}{\underline{k}_{F1}} \qquad (19)$$

where:

$$\underline{k}_{F1} = \frac{\underline{K}_1 d + \underline{L}_1}{\underline{M}_1} \text{ – fault current distribution network,}$$

$$\underline{K}_1 = -\underline{Z}_{1LA}(\underline{Z}_{1A} + \underline{Z}_{1B} + \underline{Z}_{1LB}),$$

$$\underline{L}_1 = \underline{Z}_{1LA}(\underline{Z}_{1A} + \underline{Z}_{1A} + \underline{Z}_{1LB}) + \underline{Z}_{1LB}\underline{Z}_{1B},$$

$$\underline{M}_1 = \underline{Z}_{1LA}\underline{Z}_{1LB} + (\underline{Z}_{1LA} + \underline{Z}_{1LB})(\underline{Z}_{1A} + \underline{Z}_{1B}).$$

Considering the boundary conditions of the single phase-to-ground faults one obtains for the fault current components:

$$\underline{I}_{F0} = \underline{b}_{F1} \underline{I}_{F1} \qquad (20)$$

where: $\underline{b}_{F1}$ – coefficient dependent on which phase is faulted:

- a-g fault: $\underline{b}_{F1} = 1$,
- b-g fault: $\underline{b}_{F1} = -0.5 - j0.5\sqrt{3}$,
- c-g fault: $\underline{b}_{F1} = -0.5 + j0.5\sqrt{3}$.

Substituting (18)–(19) into (20) yields:

$$\frac{\underline{I}_{AA0} - \underline{P}_0 \underline{I}_{AB0}}{1 - d} = \frac{\underline{b}_{F1} \underline{M}_1 \Delta \underline{I}_{AA1}}{\underline{K}_1 d + \underline{L}_1} \qquad (21)$$

The current $\underline{I}_{AB0}$, considered as unavailable, can be determined from (21) as a function of the sought distance to fault (d), the measured quantities: $\underline{I}_{AA0}$, $\Delta \underline{I}_{AA1}$ and the impedance parameters of the network. This, together with the fault location formula (12) or (16), allows for estimating the required current $\underline{I}_{AB0}$.
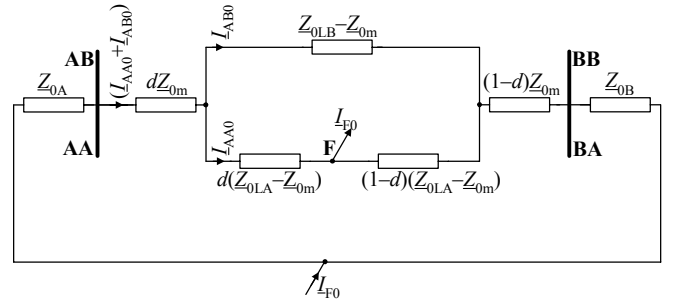
Fig. 2. Equivalent circuit diagram of the transmission network with double-circuit line for the zero-sequence
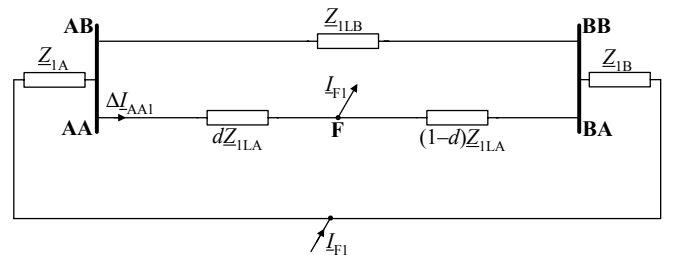
Fig. 3. Equivalent circuit diagram of the transmission network with double-circuit line for the incremental positive-sequence

IV. ATP-EMTP ALGORITHM EVALUATION

The presented algorithm has been evaluated with the fault data obtained from versatile ATP-EMTP [6] simulations of faults in the network with the 400 kV, 300 km double-circuit transmission line (the main parameters are gathered in Table III). Instrument transformers were also included in the model.

TABLE III. PARAMETERS OF THE MODELLED TRANSMISSION NETWORK

SYSTEM ELEMENT	PARAMETER	
DOUBLE-CIRCUIT LINE	Length l	300 km
	$\underline{Z}'_{1L}$	$(0.0276 + j0.315)\ \Omega/km$
	$\underline{Z}'_{0L}$	$(0.275 + j1.0265)\ \Omega/km$
	$\underline{Z}'_{0m}$	$(0.21 + j0.628)\ \Omega/km$
	$\underline{C}'_{1L}$	13 nF/km
	$\underline{C}'_{0L}$	8.5 nF/km
	$\underline{C}'_{0m}$	5 nF/km
EQUIVALENT SYSTEM A	$\underline{Z}_{1SA}$	$(2.615 + j14.829)\ \Omega$
	$\underline{Z}_{0SA}$	$(4.637 + j26.297)\ \Omega$
	Voltage phase angle	0°
EQUIVALENT SYSTEM B	$\underline{Z}_{1SB}$	$\underline{Z}_{1SB} = 2\underline{Z}_{1SA}$
	$\underline{Z}_{0SB}$	$\underline{Z}_{0SB} = 2\underline{Z}_{0SA}$
	Voltage phase angle	-30°

Different specifications of faults and pre-fault power flows have been considered in the evaluation of the accuracy of the developed fault location algorithm.

The specifications of the fault example (Fig. 4–Fig. 5) are as follows: a-b-g fault, fault distance: d=0.9 p.u., fault resistance: R_F=10 Ω. The waveforms of the measured currents and voltages are shown in Fig. 4, while the obtained results are presented in Fig. 5: the estimated distance to fault and fault resistance. Averaging within the fault interval $(30 \div 50)$ms was applied. For this fault, the estimated distance to fault with taking into account the lumped parameter line model is determined with the error exceeding 3% (d^0=0.9313 p.u.). However, applying the distributed parameter line model, the error undergoes substantial decreasing. After performing two iterations, the error is around 0.2% ($d^{2iter.}$=0.9021 p.u.).

Selected results of the fault location accuracy for different fault specifications are presented in Table IV. It is considered that the location is performed from both line sides – to consider different pre-fault power flows. The error is determined for the case the lumped line model (Error^0) and for the distributed parameter line model – after the second iteration of the calculations (Error$^{2iter.}$). It has been checked that performing two iterations is enough for getting accurate fault location results. If the distance to fault, counted from a particular line side, is higher than 0.7 p.u. (210 km) the fault location error under using the lumped line model is basically higher than 1%, exceeding even 3%. However, after applying the iterative calculations according to the distributed parameter line model, the error substantially decreases. Further reduction of errors can be achieved by applying advanced digital filtering, instead of the applied standard Fourier filtration.
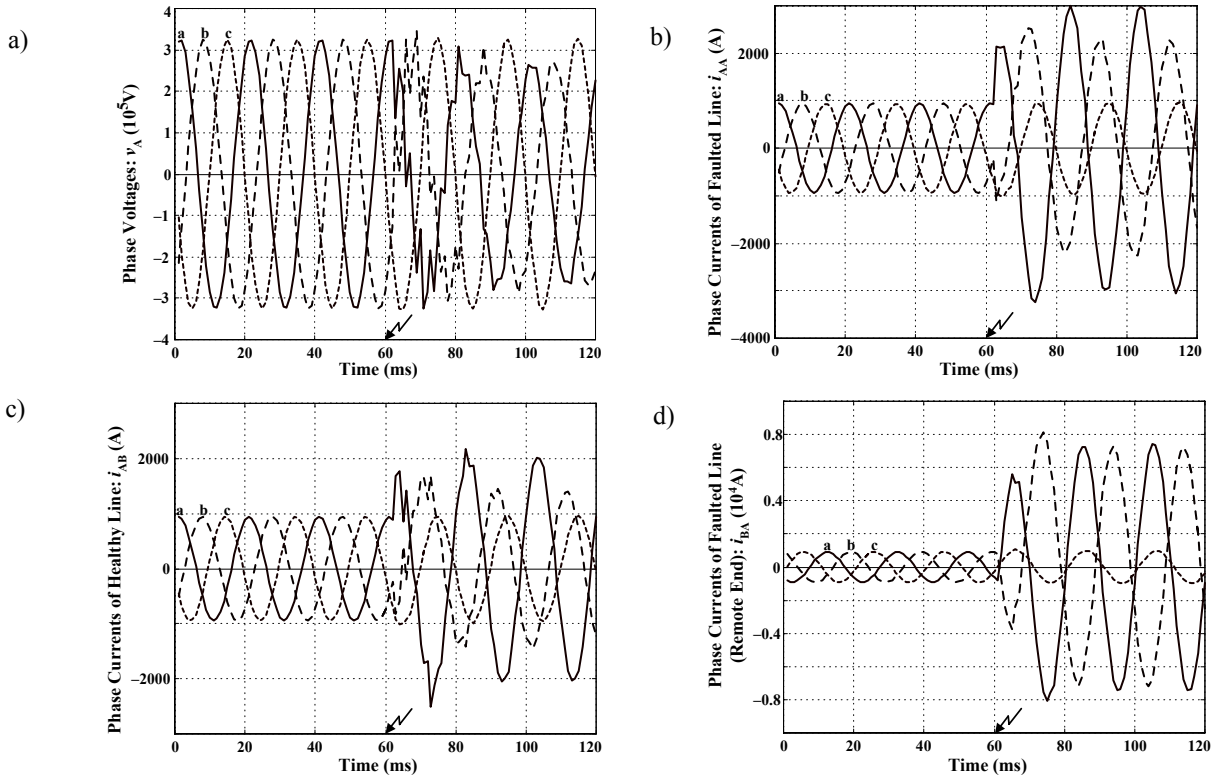
Fig. 4. The example − waveforms of signals: a) local phase voltages, b) local phase currents from faulted line, c) local phase currents from healthy line, d) remote phase currents from faulted line

a)

b)

$$R_{F\_(30\div50)ms}^0 = 10.06\ \Omega$$

$$d_{(30\div50)ms}^0 = 0.9313\ \text{p.u.}$$
$$d_{(30\div50)ms}^{2iter.} = 0.9021\ \text{p.u.}$$

a^0

$d^{2iter.}$
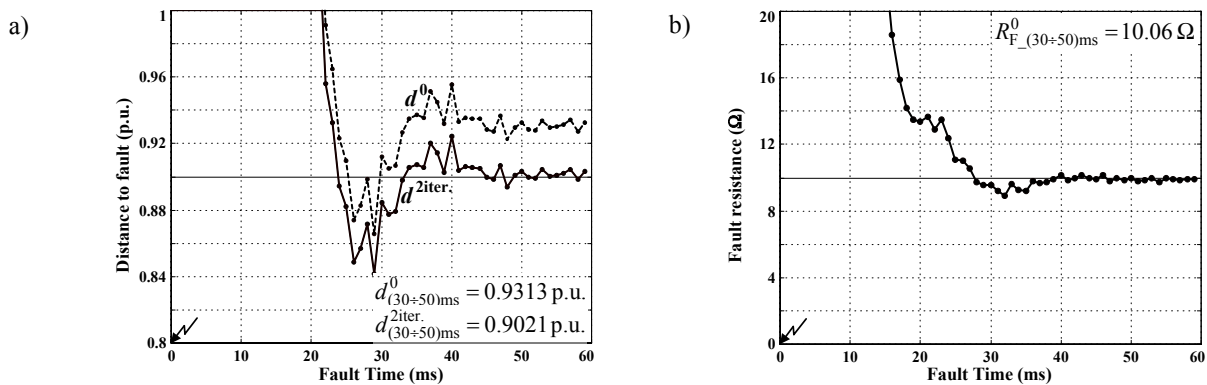
Fig. 5. The example: a) estimated distance to fault (for lumped and distributed parameter line models), b) estimated fault resistance

TABLE IV. EVALUATION OF FAULT LOCATION ERRORS

FAULT TYPE (R_F)	ACTUAL FLT DIST. (from AA)	LOCATION FROM AA		LOCATION FROM BA	
		Error^0 [%]	$\text{Error}^{2iter.}$ [%]	Error^0 [%]	$\text{Error}^{2iter.}$ [%]
a-g (R_F=10 Ω)	0.1	0.12	0.08	1.98	0.35
	0.3	0.26	0.19	1.46	0.18
	0.5	0.43	0.33	0.67	0.23
	0.7	1.78	0.64	0.32	0.19
	0.9	2.32	0.58	0.13	0.11
a-b (R_F=2 Ω)	0.1	0.02	0.02	2.95	0.15
	0.3	0.04	0.06	1.28	0.02
	0.5	0.38	0.11	0.46	0.02
	0.7	1.18	0.18	0.09	0.02
	0.9	3.02	0.04	0.01	0.01
a-b-g (R_F=10 Ω)	0.1	0.05	0.03	3.32	0.71
	0.3	0.13	0.01	1.46	0.14
	0.5	0.48	0.04	0.57	0.05
	0.7	1.29	0.09	0.10	0.02
	0.9	3.13	0.21	0.06	0.03
a-b-c (R_F=10 Ω)	0.1	0.17	0.01	1.53	0.58
	0.3	0.14	0.03	0.67	0.08
	0.5	0.17	0.06	0.13	0.03
	0.7	0.92	0.10	0.10	0.01
	0.9	2.63	0.21	0.11	0.03

V. CONCLUSIONS

The new fault location algorithm, utilising the synchronized measurements of the current differential relays has been presented. This is considered that the fault location function is incorporated into the differential relay, what assures great increase of the relay functionality. Besides indicating whether a fault occurred in a given protective zone or outside it, the relay provides also information on accurate position of the fault, which is required for the inspection-repair purpose.

The derived fault location formula is compact and covers different fault types – by setting the appropriate fault type coefficients. High accuracy of fault location is assured by taking into account the distributed parameter line model.

The ATP-EMTP based evaluation shows that the accuracy of fault location is very high under using the distributed parameter line model, for various faults and parameters of the power network.

VI. REFERENCES

[1] M. Kezunovic and B. Perunicic, *Fault location*, Wiley Encyclopedia of Electrical and Electronics Technology, New York: Wiley, 1999, vol. 7, pp. 276–285.

[2] IEEE Std C37.114: *IEEE Guide for Determining Fault Location on AC Transmission and Distribution Lines*, IEEE Power Engineering Society Publ., pp. 1–42, 8 June 2005.

[3] L. Eriksson, M.M. Saha and G.D. Rockefeller, "An accurate fault locator with compensation for apparent reactance in the fault resistance resulting from remote-end infeed", *IEEE Trans. Power Apparatus and Systems*, Vol. PAS–104, No. 2, pp. 424–436, February 1985.

[4] J. Izykowski, E. Rosolowski and M.M. Saha, "A new fault location algorithm for use with current differential protective relays of two-terminal line", *16th Power Systems Computation Conference*, 14–18.07.2008, Glasgow.

[5] J. Izykowski, E. Rosolowski and M.M. Saha, "Locating faults in parallel transmission lines under availability of complete measurements at one end", *IEE Generation, Transmission and Distribution*, Vol. 151, No. 2, pp. 268–273, 2004.

[6] H.W. Dommel, *Electro-Magnetic Transients Program*, BPA, Portland, Oregon, 1986.

VII. BIOGRAPHIES

Eugeniusz Rosolowski (M'1997, SM'00) received his M.Sc. degree in Electrical Eng. from the Wroclaw University of Technology in 1972. From 1974 to 1977, he studied in Kiev Politechnical Institute and received Ph.D. in 1978. In 1993 he received D.Sc. from the WrUT. Presently he is a Professor in the Institute of Electrical Engineering. His research interests are in power system analysis and relaying algorithms.

Jan Izykowski (SM'04) received his M.Sc., Ph.D. and D.Sc. degrees from the Faculty of Electrical Engineering of the Wroclaw University of Technology (WrUT) in 1973, 1976 and in 2001, respectively. In 1973 he joined Institute of Electrical Engineering of the WrUT, where presently he is a Professor. His research interests are in power system protection and control, power system simulation, transient performance of instrument transformers, and fault location.

Murari Mohan Saha (M´76–SM´87) was born in 1947 in Bangladesh. He received B.Sc. E.E. and M.Sc. E.E. from Bangladesh University of Engineering and Technology (BUET), Dhaka, Bangladesh, in 1968 and 1970 respectively. In 1975 he received Ph.D. from the Technical University of Warsaw, Poland. Currently he is a Senior Research and Development Engineer at ABB AB, Västerås, Sweden. His areas of interest are power system simulation, instrument transformers and digital protective relays.